Impact of inhaled nitric oxide on white matter damage in growth-restricted neonatal rats

Hoa Pham[1,2], An Phan Duy[1,2], Julien Pansiot[1,2], Bieke Bollen[1,2], Jorge Gallego[1,2], Christiane Charriaut-Marlangue[1,2] and Olivier Baud[1–3]

BACKGROUND: Fetal growth restriction is the second leading cause of perinatal morbidity and mortality, and neonates with intrauterine growth retardation (IUGR) have increased neurocognitive and neuropsychiatric morbidity. These neurocognitive impairments are mainly related to injury of the developing brain associated with IUGR. Growing evidence from preclinical models of brain injury in both adult and neonatal rodents supports the view that nitric oxide can promote neuroprotection.

METHODS: In a model of IUGR induced by protracted gestational hypoxia leading to diffuse white matter injury, we subjected neonatal rats to low dose (5 ppm) but long-lasting (7 d) exposure to inhaled NO (iNO). We used a combination of techniques, including immunohistochemistry, quantitative PCR, and cognitive assessment, to assess neuroprotection.

RESULTS: Antenatal hypoxia-induced IUGR was associated with severe neuroinflammation and delayed myelination. iNO exposure during the first postnatal week significantly attenuated cell death and microglial activation, enhanced oligodendroglial proliferation and finally improved myelination. Remarkably, iNO was associated with the specific upregulation of P27kip1, which initiates oligodendrocytic differentiation. Finally, iNO counteracted the deleterious effects of hypoxia on learning abilities.

CONCLUSION: This study provides new evidence that iNO could be effective in preventing brain damage and/or enhancing repair of the developing brain.

Fetal growth restriction is the second cause of perinatal morbidity and mortality after prematurity, and occurs in 5–12% of all pregnancies in the general population (1,2). Neonates born after a pregnancy complicated by intrauterine growth retardation (IUGR) have increased neurocognitive and neuropsychiatric morbidity (3,4). Indeed, fetal growth restriction has been associated with a three- to fivefold increase in cerebral palsy in term and near-term infants (5), and infants born with growth restriction are more likely to display neurocognitive dysfunctions and poor school performance (6,7), and to develop behavioral and psychiatric disorders (8,9). Finally, IUGR is associated with memory, attention, and executive deficits, regardless of prematurity or socioeconomic factors (7,10).

Several of these neurocognitive impairments are associated with the IUGR-related injury of the developing brain. Specifically, white matter damage, the most common form of perinatal brain injury, is considered the leading cause of long-term handicap in neonates (11). It is related to a maturation-dependent vulnerability of the oligodendrocyte lineage to several risk factors, including hypoxia and ischemia, maternal-fetal infection, and IUGR (12). In addition to white matter, gray matter has been found to be altered following fetal growth restriction (13).

Recently, we reported that the nitric oxide pathway is able to promote oligodendroglial maturation, myelination, and neuroprotection in preclinical models of neonatal stroke and white matter damage induced by postnatal hyperoxia or excitotoxic insult (14–18). Several other reports have demonstrated that inhaled NO (iNO) is associated with significant neuroprotection in preclinical models of adult brain damage (19–22).

Here, we have investigated the effect of iNO in a model of IUGR induced by protracted gestational hypoxia leading to diffuse white matter injury (23).

RESULTS

iNO Reduces IUGR-Associated Brain Injury Induced by Antenatal Hypoxia

Body weight and postnatal mortality were measured in pups on P3 and P10 (**Supplementary Table S1** online). Combining data from more than 10 litters, antenatal hypoxia resulted in a pronounced restriction in body weight and increased mortality. iNO exposure during delivery and within the first week of life was able to significantly improve catch up on P3 and P10 and led to an increased survival rate. Antenatal hypoxia-induced IUGR was associated with a significant increase in the density of cell death detected within the hemispheric periventricular white matter using either cleaved caspase 3 (CC3) labeling or terminal deoxynucleotidyl transferase nick-end labeling (TUNEL) on P3 (**Figure 1a**,**b**). Exposure to 5 ppm iNO significantly reduced this deleterious effect as measured by TUNEL. Interestingly, double immunolabeling showed that CC3/O4 double positive cells density within the developing white matter was significantly increased in air-exposed IUGR rat pups at P3 but was found similar to

[1]INSERM UMR1141, Université Paris Diderot, Paris, France; [2]PremUP Foundation, Paris, France; [3]Neonatal Intensive Care Unit, Robert Debré Children's Hospital, Assistance Publique – Hôpitaux de Paris, Paris, France. Correspondence: Olivier Baud (olivier.baud@rdb.aphp.fr)

Received 7 March 2014; accepted 30 September 2014; advance online publication 4 February 2015. doi:10.1038/pr.2015.4

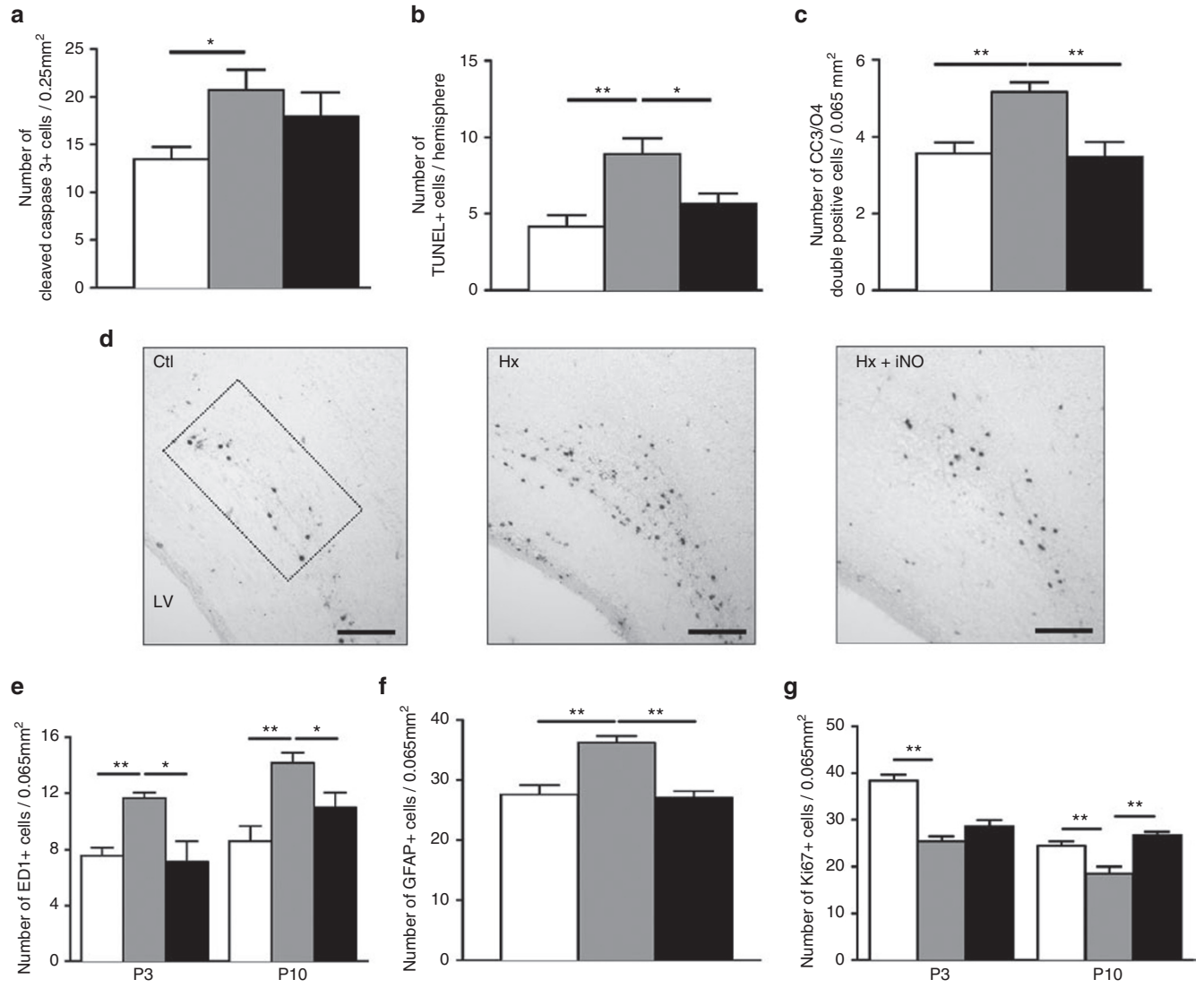

Figure 1. Impact of inhaled NO (iNO) on main features of brain injury associated with intrauterine growth retardation in rat pups. (**a–c**) Quantitative analysis of the density of cleaved caspase-3-positive cells (**a**) and total terminal deoxynucleotidyl transferase nick-end labeling–positive cells per hemisphere (**b**) and cleaved caspase 3 (CC3)/O4 double positive cell density (**c**) within the WM, in P3 growth-restricted rat pups with (black bars) or without (gray bars) exposure to iNO, compared to controls (Ctl, white bars). (**d–e**) Representative photomicrographs (**d**) and quantitative analysis (**e**) and of ED1-positive cells in the cingulate WM in P3 growth-restricted rat pups with (black bars) or without (gray bars) exposure to iNO, compared to controls (Ctl, white bars). LV, lateral ventricle. Scale bar = 100 µm. (**f,g**) Quantitative analysis of glial fibilllary acidic protein (GFAP)-positive cells (**a**) in P3 rat pups, and Ki67-positive cells (**b**) in the cingulate WM in P3 and P10 rat pups subjected to gestational hypoxia with (black bars) or without (gray bars) exposure to iNO, compared to controls (Ctl, white bars). For all, $*P < 0.05$, $**P < 0.01$ for comparisons between the groups indicated using one-way ANOVA with Dunnett's correction.

control animals in iNO-exposed rat pups (Figure 1c). In contrast, no effect has been detected in either CC3/PS100 or CC3/NeuN double positive cells density within the developing white matter and cortex, respectively (**Supplementary Figure S1** online).

Increased microglial activation within the developing white matter was observed in growth-restricted P3 and P10 pups but not in pups exposed to iNO (Figure 1d,e). Similarly, the density of glial fibilllary acidic protein-positive cells in the cingulate white matter was found to be increased in IUGR pups exposed to room air but not in those exposed to iNO (Figure 1f). Finally, IUGR pups were characterized by a reduction in the density of proliferating cells as assessed using labeling for Ki67 (Figure 1g). iNO had significant effect on cell proliferation of oligodendroglial cells in P3 pups as shown in **Supplementary Figure S2** online.

iNO and Oligodendroglial Lineage in IUGR Pups

We next asked whether iNO could modify oligodendroglial maturation in IUGR pups. Antenatal hypoxia induced a significant decrease in the density of NG2-immunolabeled immature oligodendrocytes in the white matter at P3 (Figure 2a). Postnatal exposure to iNO was unable to attenuate this effect. In contrast, iNO increased the mature oligodendrocytes density observed in growth-restricted pups subjected to antenatal hypoxia, as measured by immunoreactivity to adenomatous polyposis Coli (APC) (Figure 2b). At P10, the density of myelinated (myelin basic protein (MBP)-positive) fibers

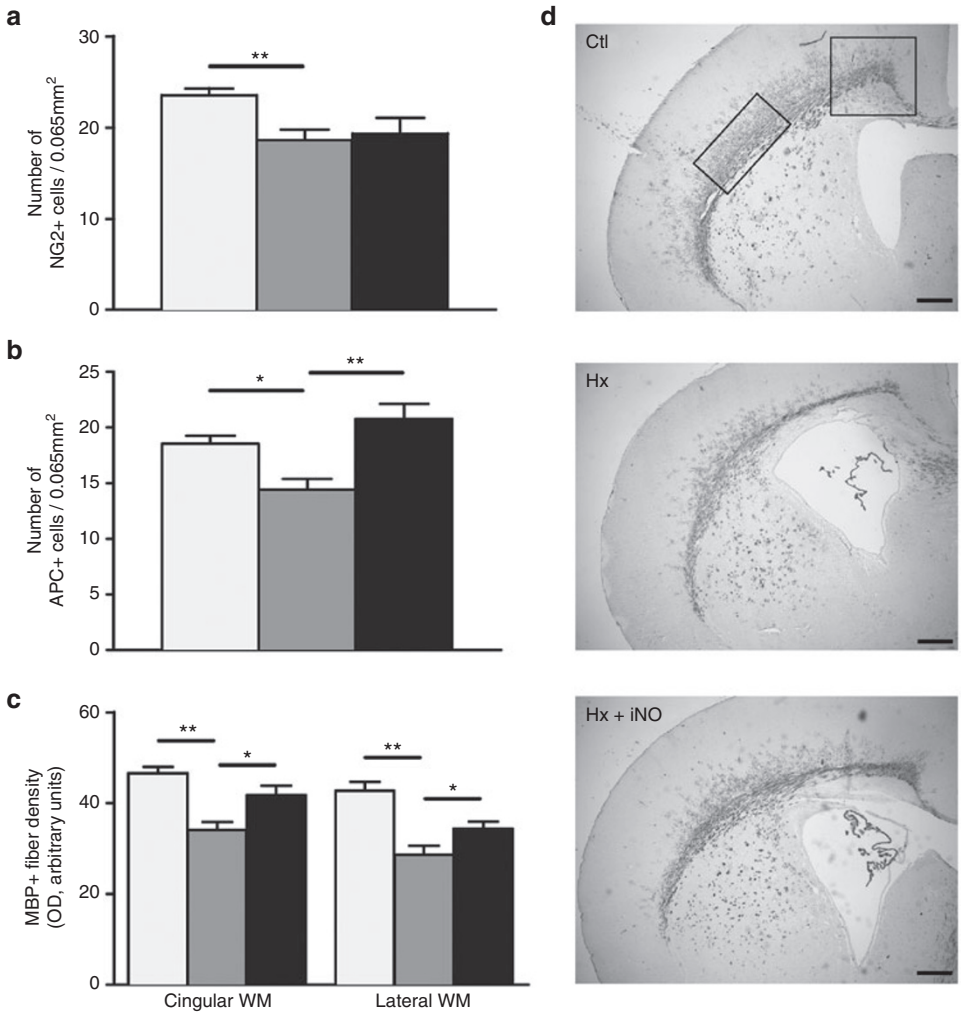

Figure 2. Impact of inhaled NO (iNO) on oligodendroglial cell maturation in intrauterine growth retardation (IUGR) rat pups. (**a**) Quantitative analysis of NG2-positive cells in the cingulate WM in P3 growth-restricted rat pups with (black bars) or without (gray bars) exposure to iNO, compared to controls (Ctl, white bars). (**b**) Quantitative analysis of APC-positive cells in the cingulate WM in P10 growth-restricted rat pups with (black bars) or without (gray bars) exposure to iNO, compared to controls (Ctl, white bars). (**c,d**) Quantitative analysis of the optical density of MBP-positive fibers in the cingulate and lateral white matter in P10 growth-restricted rat pups with (black bars) or without (gray bars) exposure to iNO, compared to controls (Ctl, white bars). These data demonstrate that myelin content is deficient in IUGR-pups compared to controls (Ctl). In contrast, low dose (5 ppm) iNO exposure restored the optical density of MBP-positive fibers to levels similar to those in controls. Scale bar = 200 µm. For all, $*P < 0.05$, $**P < 0.01$ for comparisons between the groups indicated using one-way ANOVA with Dunnett's correction.

in IUGR pups exposed to iNO was found restored to normal levels, in both the cingulate and lateral white matter (Figure 2c,d). These findings were gender-independent.

Since the oligodendroglial lineage is regulated by several transcription factors, we next used quantitative PCR analysis to evaluate expression levels of the following factors in P3 and P10 pups: PDGFRα, a marker of proliferating oligodendrocyte progenitors; P27kip1, a promaturation factor; and Sox10, which stimulates p27kip1-induced MBP expression. IUGR was associated with a significant reduction in the expression levels of both P27kip1 and Sox10, and a nonsignificant decrease in the expression level of PDGFRα in P3 rat pups (Figure 3a–c). In contrast, the expression levels of PDGFRα, P27kip1 and Sox10 were similar or higher than in controls in IUGR pups exposed to iNO, suggesting that iNO triggered a compensatory increase in their expression. The effects of antenatal-hypoxia-induced IUGR, however, appear to have been transient, as most changes observed at P3 were no longer statistically significant or were less marked at P10.

Because white matter damage could induce axonal degeneration, we investigated P10 rat pups using fractin immunostainings. Fractin has been reported as a reliable marker for detecting reactive astrocytes and the diffuse gliotic component of periventricular leukoamalacia (24). We found scattered but numerous fractin-positive astrocytic-like cells as well as fibers in the white matter in IUGR rat pups. In contrast, almost no reactivity was noted in iNO-treated animals (**Supplementary Figure S3** online).

iNO Prevents IUGR-Associated Behavioral Disorders

Finally, we asked whether IUGR induced by protracted gestational hypoxia could have a functional impact on learning

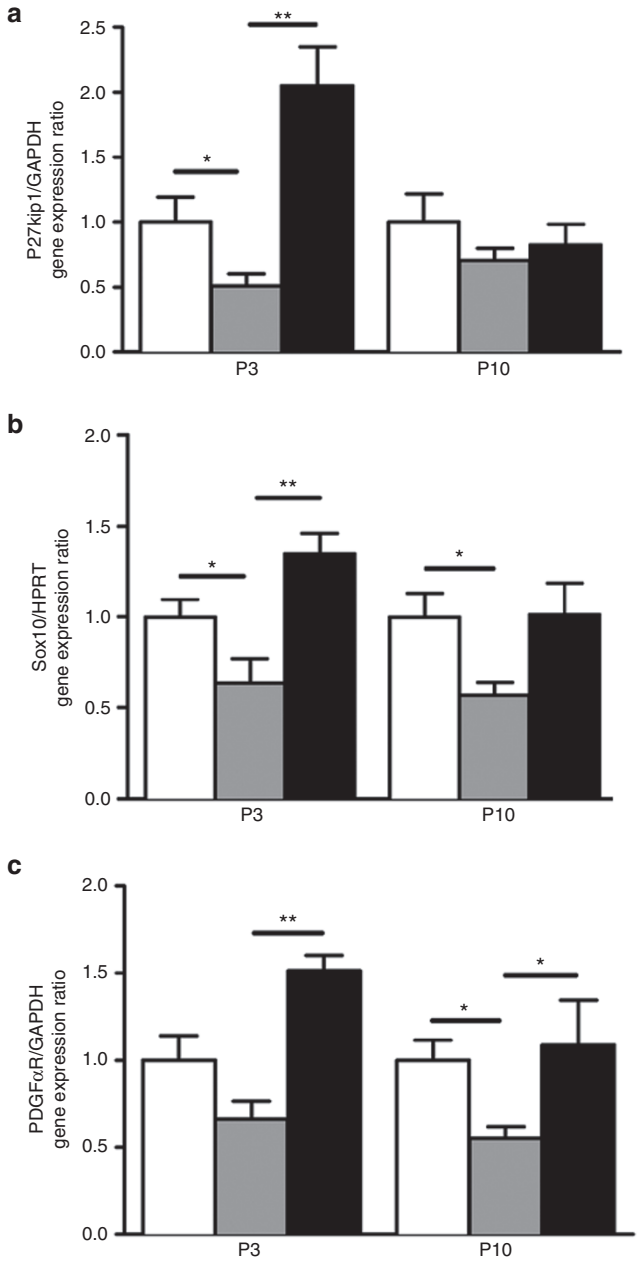

Figure 3. Impact of inhaled NO (iNO) on the expression of transcription factors involved in oligodendroglial maturation and myelination in intrauterine growth retardation rat pups. (**a–c**) Quantitative analysis of gene expression levels of p27kip1 (**a**), PDGFαR (**b**) and sox10 (**c**) in P3 and P10 growth-restricted rat pups with (black bars) or without (gray bars) exposure to iNO, compared to controls (Ctl, white bars). For all, $^{*}P < 0.05$, $^{**}P < 0.01$ for comparisons between the groups indicated using one-way ANOVA with Dunnett's correction.

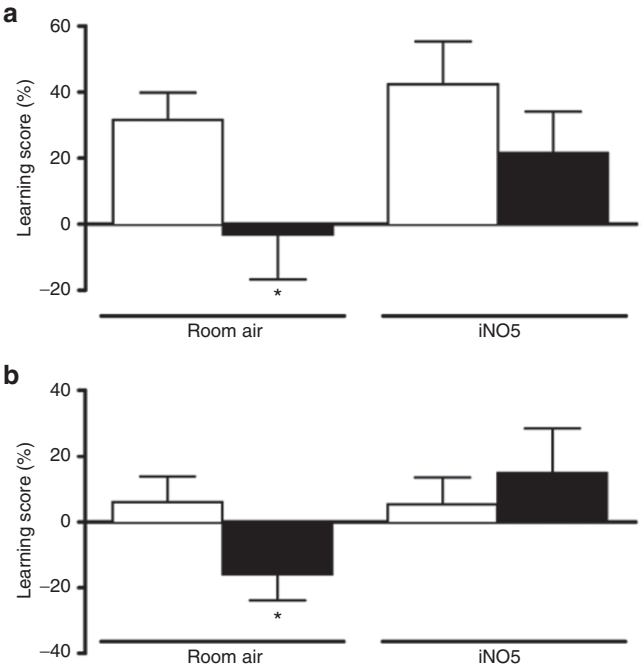

Figure 4. Impact of inhaled NO (iNO) on odor preference conditioning test scores. Associative learning scores at P3 (**a**) and P10 (**b**) in rat pups subjected to antenatal hypoxia (black bars) or controls (white bars), with or without exposure to iNO. Gestational hypoxia abolished learning ability at both ages while iNO treatment improved learning scores in intrauterine growth retardation rat pups to levels similar to those in controls. $^{*}P < 0.05$ compared to control scores, unilateral *t*-test.

abilities. Olfactory conditioning experiments, which allow the detection of early dysfunctions in associative memory, were performed with P3 and P10 rat pups (**Figure 4a**,**b**). These experiments showed that IUGR pups were characterized by a marked learning deficit, irrespective of age. iNO exposure did not modify behavioral performance in control pups. In contrast, iNO exposure significantly improved associative learning abilities in growth-restricted pups, to a level similar to that in normal pups.

DISCUSSION

In this study, we explored an animal model that mimics IUGR by exposing pregnant rats to protracted gestational hypoxia. In this model, pups born to dams exposed to hypoxia showed significantly reduced body weight and increased mortality, as well as IUGR-associated WMD, including neuroinflammation and delayed myelination in the neonatal period. However low-dose (5 ppm) iNO exposure during the first postnatal week significantly attenuated these principal features. The main beneficial effects induced by iNO were decreased cell death, reduced microglial activation, enhancement of oligodendroglial proliferation, and finally improved myelination. Remarkably, iNO was associated with the specific upregulation of three genes related to an increased number of proliferating Olig2 positive cells, PDGFRα, P27kip1 and Sox10. Finally, iNO counteracted the deleterious effects of hypoxia on learning abilities, restoring associative learning scores to the normal range.

This study emphasizes the impact of antenatal growth retardation on brain development and postnatal brain damage. Fetal exposure to nutrient or oxygen restriction leads to changes in many mechanisms involved in energy metabolism, cell structure and neurotransmission, and thus on overall brain development (25). The concept of disruption of the developmental program may interfere with the subsequent occurrence

of multiple disabilities, behavioral changes, and brain plasticity (26).

In our model, microglial activation following fetal growth restriction is also consistent with recent reports demonstrating that infants with IUGR appear to be at increased risk of systemic inflammation postnatally (27). Thus, this two-hit model of brain damage, combining the effects of IUGR and systemic postnatal inflammation is clinically relevant, as IUGR along with a synergistic effect of systemic inflammation places very preterm human newborns at increased risk for a low mental development index (28). The concept of inflammation-induced sensitization is emerging in the field of perinatal brain injury, and chronic inflammation could disrupt several developmental programs in the central nervous system, including oligodendroglial lineage blockade, maturation disruption, and myelination process (29). In several recent reports, oligodendroglial maturation arrest has been definitively shown in hypoxia ischemia models and in human pathology (30–32). Although preoligodendrocytes are vulnerable to cell death acutely, they subsequently proliferate after injury. In our study, postnatal iNO exposure appears to restore cell proliferation reduced after antenatal hypoxia. Despite the increased numbers, preoligodendroglial cells do not go on to produce myelinating mature oligodendrocytes because of maturation arrest in which chronic inflammation play a key role (33). Here we found that iNO can prevent white matter inflammation and its consequences on myelination, suggesting that the blockade of the developmental program of the white matter can be reversed.

The effects of exposure to iNO reported here are consistent with our previous work demonstrating that both endogenous and exogenous (inhaled) NO affect myelination in normal rodent pups (14). Recently, we have demonstrated that iNO has a neuroprotective effect on white matter injury following excitotoxic insult (15) or perinatal oxidative stress (18). These data demonstrate that low doses of iNO act not only locally on the pulmonary vasculature, but have a remote impact on the normal and injured developing brain. How iNO is transported from the lung to the brain remains to be elucidated, although one possibility are that it could be carried by the blood in a bioactive format in association with several potential NO carriers including S-nitroso-hemoglobin, S-nitrosothiols, and nitrite. Once in the brain, Terpollili *et al.* (21) have suggested that bioactive NO could be released via an oxygen-tension-dependent mechanism.

The idea that exogenous NO could be neuroprotective in perinatal brain damage is fairly controversial. Several studies have demonstrated the deleterious effects of reactive nitrogen species accumulation following ischemia-reperfusion brain injury, through mechanisms ranging from energy failure, lipid peroxidation, protein nitrosylation, and DNA alterations to increased permeability of the blood–brain barrier (34). The immature brain is especially vulnerable to damage by acute/chronic inflammation and oxidative stress. On the other hand, growing evidence demonstrates that iNO and NO-pathway-derived molecules could have a beneficial effect, depending on its concentration and the time-period of exposure following the insult (16,17). In our model, oxidative stress is likely not the prominent mechanism of injury as the antenatal intervention is hypoxia. In contrast, postnatal inflammation potentiated by antenatal growth restriction could be attenuated through circulating NO derivatives during the first week of life and its vascular and cellular effects. Recently, Akt/eNOS pathway has been shown to mediate anti-inflammatory activity in TBI-injured brain (35). In addition to iNO, other therapeutic strategies influencing NO signaling, especially those that improve cerebral blood flow or modulate inflammation using NO donors or NOS inhibitors, have been proposed to restore NO signaling in the mature brain. However, NOS inhibitors are not currently in use clinically due to their deleterious side effects. In adults, some NO-derived therapeutic approaches for stroke prevention, such as the use of statins (HMG-CoA reductase inhibitors), have been implemented in clinical practice (36), but stroke treatments involving Rho-kinase (ROCK) inhibitors, phosphodiesterase inhibitors, the PI3Kinase/Akt pathway or NOS-3 activation are still at the experimental stage, and require more work before a side-effect-free molecule or strategy can be proposed (21). Recently, we have reported that sildenafil citrate, a phosphodiesterase-5 inhibitor, induces a significant increase in cerebral blood flow and reduces hypoxic ischemic brain damage in neonatal rats (37).

In conclusion, this study provides new evidence that iNO could be effective in preventing damage and/or enhancing repair in a preclinical rat model of perinatal brain injury. Further investigations are needed to explore mechanistic aspects of the effect of exogenous NO on the oligodendroglial lineage.

METHODS

Experimental Protocol and Gas Exposure

This study was approved by the French National Institute of Health and Medical Research and complied with the guidelines of the Institutional Animal Care and Use Committee of INSERM 1141, Paris.

Pregnant Sprague-Dawley rats (Charles River Laboratories, L'Arbresle, France) were placed in normoxic or hypoxic (10% O_2–90% N_2) gas chambers (Biospherix, Redfield, NY) from embryonic day (E) 5 to 19 as previously described (23). Oxygen concentration was monitored using a Proox device (Biospherix). CO_2 concentration was consistently kept under 0.1%. To investigate the impact of exogenous NO on the developing brain and lung, low-concentration iNO (5 ppm) was introduced into the chambers 12–24 h prior to delivery and up to postnatal day (P) 7 and monitored using an iNOvent system (INOTherapeutics, Clinton, NJ). The NO_2 concentration was kept under 1 ppm. In the control group, animals were kept in room air after delivery. From P7 up to sacrifice, rat pups and their mothers in all experimental groups were kept in room air. Animals were housed under controlled temperature (22 ± 1 °C) and light conditions (12 h day/night cycle) with food and water *ad libitum*. Neonatal mortality was checked daily.

Tissue Preparation

Pups were sacrificed at P3, P10, or P21 (n = 7–9/group for each histological protocol). Two distinct fixation protocols were used:

(i) Brains were directly removed and immersed in 4% formol and embedded in paraffin.
(ii) Pups were perfused transcardially with 4% paraformaldehyde in phosphate buffer (0.12 M, pH 7.4). Brains were equilibrated with 10% sucrose in phosphate buffer for 2–4 d, frozen in liquid-nitrogen-cooled isopentane, stored at −80 °C and cut coronally into serial 10-µm-thick sections.

Immunohistochemistry

Primary antibodies used in this study are listed in **Supplementary Table S2** online. All quantification of immunoreactive cells was carried out by investigators blind to the experimental groups.

For brain immunohistochemistry, coronal sections (+1.44 to −0.48 mm from bregma) were selected and processed as previously described (14). In each experimental group, we studied seven to eight pups in three separate experiments. Immunolabeling was visualized using the streptavidin-biotin-peroxidase method. Double-labeling was performed with secondary antibodies coupled to the green fluorescent marker Fluoroprobe S488 (Interchim, Montluçon, France) or the red fluorescent marker cyanine 3 (Jackson Immunoresearch laboratories, West Grove, PA).

Optical Density of Myelinated and Axonal Fibers

The optical density of MBP-stained immunoreactive fibers was measured in two different regions (cingulum and lateral corpus callosum) as previously described (38), using a computerized image-analysis system (Image J 1.41o, National Institutes of Health, Bethesda, MD) that reads optical density as gray levels. Four sections per brain were examined for each animal at P10. Nonspecific background densities were measured at each brain level in a region devoid of MBP-positive fibers immunolabeling, and were subtracted from values of the region of interest.

TUNEL Assay

Apoptotic cells in the white matter at P3 were detected using the TUNEL assay (In Situ Cell Death Detection Kit, Roche, Meylan, France) according to the manufacturer's instructions. Labeled cell nuclei were counted in four sections for each hemisphere on images captured with a 40× objective.

Western Blotting

Snap-frozen brain cortices including white matter were subjected to different protocols to separate nuclear proteins, cytosolic proteins, and mitochondrial proteins. Proteins (40 µg) were separated on 10% polyacrylamide gels, using Ponceau-S staining and β-actin as the loading standard for cytosolic proteins, and histone-3 as the loading standard for nuclear proteins. Bands were transferred to membranes, which were incubated in primary antibodies diluted in blocking buffer (rabbit polyclonal anti-AIF, rabbit polyclonal anti-cleaved caspase-3, or mouse monoclonal anti-cytochrome C) overnight at 4 °C. They were then incubated with a secondary antibody (horseradish peroxidase–linked anti-rabbit or anti-mouse: 1/5,000) for 1.5 h at room temperature, and positive signals visualized using WesternC chemiluminescence (Bio-Rad, Marnes-la-Coquette, France). Western blots were performed in triplicate using samples from 4–6 animals per group.

RT-PCR

Total mRNA was isolated using the RNeasy Lipid Tissue kit (Qiagen, Courtaboeuf, France) according to the manufacturer's instructions and as previously reported (34). cDNA was produced from 600 ng of total mRNA by reverse transcription with the Iscript kit (Bio-Rad). Sequences for the forward and reverse oligonucleotide primers, designed with the Primer Express software package (Life Technologies SAS, Saint Aubin, France), are listed in **Supplementary Table S3** online. Each experiment was run twice with eight animals per group, and in both cases, measurements were carried out in triplicate. Values are expressed relative to the levels of housekeeping genes (GAPDH or HPRT).

Cognitive Assessment

Associative abilities were assessed at P3 and P10 using an odor preference conditioning test. In this test, the pups learn to associate two artificial odors with either warm (34 °C) or cold (26 °C) temperature (the CS+ and the CS− odor, respectively). First, during the acquisition phase, the pups were placed in contact with one odor (either peppermint, 0.5 ml 97% menthyl acetate, or banana 97% butyl propionate, Aldrich, Steinheim, Germany) for 30 s. The exposure to each odor paired with either warm or cold temperature was carried out using custom exposure chambers, as follows. The chambers were composed of a small cylindrical mesh cage (diameter: 16 cm, height: 21 cm) surrounding the odor-containing cotton wad and secured in a metal box immersed in a thermoregulated water bath. To control for initial differences in preference between the two odors, for half the pups, banana was paired with warm temperature and peppermint with cold temperature, and vice versa in the other half. The pups were randomly assigned to the peppermint CS+ or to the banana CS+ group.

Immediately after acquisition, the pups underwent a two-odor choice test in cold conditions using a previously described setup (39). Briefly, two boxes were placed 2 cm apart, each containing an odor-impregnated cotton wad, and covered by a 13 × 20 cm metallic mesh floor. During each test (duration: 60 s, five tests), the pup was initially placed on the 2-cm wide neutral zone. Then, as the pup walked around the mesh floor, the experimenter measured the time spent over each odor (i.e., time on CS+ and time on CS−). The temperature of the test apparatus was maintained at 24 °C to motivate the pups to search for warmth. A pup was considered to prefer an odor when it moved at least its snout toward the odor, beyond the edge of the neutral zone. The orientation in which the pup was placed on the neutral line was changed (i.e., 180° rotation) at the beginning of each test. A preference score was calculated as: 100 × (time on CS+ − time on CS−)/(time on CS+ + time on CS−). Effective learning was considered to have occured in a given group if the mean learning score was significantly above zero.

Statistical Analysis

Values are expressed as means ± SEM. Statistical comparisons between normoxic control and exposed groups were performed using one-way ANOVA followed by a Dunnett's multiple comparison test. Pairwise comparisons between groups with or without iNO exposure were done using the Mann–Whitney *U*-test. Statistical tests were run on Prism version 5.01 (GraphPad Software, San Diego, CA) and StatView version 5.0 for Mac OS (Abacus Concepts, Berkeley, CA).

SUPPLEMENTARY MATERIAL

Supplementary material is linked to the online version of the paper at http://www.nature.com/pr

STATEMENT OF FINANCIAL SUPPORT

This study was funded by INSERM (Institut National de la Santé et de la Recherche Médicale), and Premup Foundation. The funders had no role in study design, data collection and analysis, decision to publish, or preparation of the manuscript. We have nothing to disclose.

REFERENCES

1. Gabbe SG, Niebyl JR, Simpson JL, et al. Intrauterine growth restriction. In: Gabbe SG, Niebyl JR, Simpson JL, et al, eds. *Obstetrics: Normal and Problem Pregnancies*. 3rd edn. New York: Churchill Livingstone, 1996:863–86.
2. Neerhof MG. Causes of intrauterine growth restriction. Clin Perinatol 1995;22:375–85.
3. Hack M, Flannery DJ, Schluchter M, Cartar L, Borawski E, Klein N. Outcomes in young adulthood for very-low-birth-weight infants. N Engl J Med 2002;346:149–57.
4. Ozanne SE, Fernandez-Twinn D, Hales CN. Fetal growth and adult diseases. Semin Perinatol 2004;28:81–7.
5. Jarvis S, Glinianaia SV, Torrioli MG, et al.; Surveillance of Cerebral Palsy in Europe (SCPE) collaboration of European Cerebral Palsy Registers. Cerebral palsy and intrauterine growth in single births: European collaborative study. Lancet 2003;362:1106–11.
6. O'Keeffe MJ, O'Callaghan M, Williams GM, Najman JM, Bor W. Learning, cognitive, and attentional problems in adolescents born small for gestational age. Pediatrics 2003;112:301–7.

7. Geva R, Eshel R, Leitner Y, Fattal-Valevski A, Harel S. Memory functions of children born with asymmetric intrauterine growth restriction. Brain Res 2006;1117:186–94.
8. Wiles NJ, Peters TJ, Heron J, Gunnell D, Emond A, Lewis G. Fetal growth and childhood behavioral problems: results from the ALSPAC cohort. Am J Epidemiol 2006;163:829–37.
9. Cannon M, Jones PB, Murray RM. Obstetric complications and schizophrenia: historical and meta-analytic review. Am J Psychiatry 2002;159:1080–92.
10. Isaacs EB, Lucas A, Chong WK, et al. Hippocampal volume and everyday memory in children of very low birth weight. Pediatr Res 2000;47:713–20.
11. Ferriero DM. Neonatal brain injury. N Engl J Med 2004;351:1985–95.
12. Volpe JJ. Brain injury in premature infants: a complex amalgam of destructive and developmental disturbances. Lancet Neurol 2009;8:110–24.
13. Batalle D, Eixarch E, Figueras F, et al. Altered small-world topology of structural brain networks in infants with intrauterine growth restriction and its association with later neurodevelopmental outcome. Neuroimage 2012;60:1352–66.
14. Olivier P, Loron G, Fontaine RH, et al. Nitric oxide plays a key role in myelination in the developing brain. J Neuropathol Exp Neurol 2010;69:828–37.
15. Pansiot J, Loron G, Olivier P, et al. Neuroprotective effect of inhaled nitric oxide on excitotoxic-induced brain damage in neonatal rat. PLoS One 2010;5:e10916.
16. Charriaut-Marlangue C, Bonnin P, Gharib A, et al. Inhaled nitric oxide reduces brain damage by collateral recruitment in a neonatal stroke model. Stroke 2012;43:3078–84.
17. Charriaut-Marlangue C, Bonnin P, Pham H, et al. Nitric oxide signaling in the brain: a new target for inhaled nitric oxide? Ann Neurol 2013;73:442–8.
18. Pham H, Vottier G, Pansiot J, et al. Inhaled NO prevents hyperoxia-induced white matter damage in neonatal rats. Exp Neurol 2014;252:114–23.
19. Terpolilli NA, Kim SW, Thal SC, et al. Inhalation of nitric oxide prevents ischemic brain damage in experimental stroke by selective dilatation of collateral arterioles. Circ Res 2012;110:727–38.
20. Terpolilli NA, Kim SW, Thal SC, Kuebler WM, Plesnila N. Inhaled nitric oxide reduces secondary brain damage after traumatic brain injury in mice. J Cereb Blood Flow Metab 2013;33:311–8.
21. Terpolilli NA, Moskowitz MA, Plesnila N. Nitric oxide: considerations for the treatment of ischemic stroke. J Cereb Blood Flow Metab 2012;32:1332–46.
22. Li YS, Shemmer B, Stone E, A Nardi M, Jonas S, Quartermain D. Neuroprotection by inhaled nitric oxide in a murine stroke model is concentration and duration dependent. Brain Res 2013;1507:134–45.
23. Baud O, Daire JL, Dalmaz Y, et al. Gestational hypoxia induces white matter damage in neonatal rats: a new model of periventricular leukomalacia. Brain Pathol 2004;14:1–10.
24. Haynes RL, Billiards SS, Borenstein NS, Volpe JJ, Kinney HC. Diffuse axonal injury in periventricular leukomalacia as determined by apoptotic marker fractin. Pediatr Res 2008;63:656–61.
25. Rees S, Harding R, Walker D. The biological basis of injury and neuroprotection in the fetal and neonatal brain. Int J Dev Neurosci 2011;29:551–63.
26. Johnston MV. Clinical disorders of brain plasticity. Brain Dev 2004;26:73–80.
27. McElrath TF, Allred EN, Van Marter L, Fichorova RN, Leviton A; ELGAN Study Investigators. Perinatal systemic inflammatory responses of growth-restricted preterm newborns. Acta Paediatr 2013;102:e439–42.
28. Leviton A, Fichorova RN, O'Shea TM, et al.; ELGAN Study Investigators. Two-hit model of brain damage in the very preterm newborn: small for gestational age and postnatal systemic inflammation. Pediatr Res 2013;73:362–70.
29. Hagberg H, Gressens P, Mallard C. Inflammation during fetal and neonatal life: implications for neurologic and neuropsychiatric disease in children and adults. Ann Neurol 2012;71:444–57.
30. Buser JR, Maire J, Riddle A, et al. Arrested preoligodendrocyte maturation contributes to myelination failure in premature infants. Ann Neurol 2012;71:93–109.
31. Segovia KN, McClure M, Moravec M, et al. Arrested oligodendrocyte lineage maturation in chronic perinatal white matter injury. Ann Neurol 2008;63:520–30.
32. Yuen TJ, Silbereis JC, Griveau A, et al. Oligodendrocyte-encoded HIF function couples postnatal myelination and white matter angiogenesis. Cell 2014;158:383–96.
33. Chhor V, Schang AL, Favrais G, Fleiss B, Gressens P. [Long-term cerebral effects of perinatal inflammation]. Arch Pediatr 2012;19:946–52.
34. Iadecola C. Bright and dark sides of nitric oxide in ischemic brain injury. Trends Neurosci 1997;20:132–9.
35. Chen W, Qi J, Feng F, et al. Neuroprotective effect of allicin against traumatic brain injury via Akt/endothelial nitric oxide synthase pathway-mediated anti-inflammatory and anti-oxidative activities. Neurochem Int 2014;68:28–37.
36. Amarenco P, Bogousslavsky J, Callahan A 3rd, et al.; Stroke Prevention by Aggressive Reduction in Cholesterol Levels (SPARCL) Investigators. High-dose atorvastatin after stroke or transient ischemic attack. N Engl J Med 2006;355:549–59.
37. Charriaut-Marlangue C, Nguyen T, Bonnin P, et al. Sildenafil mediates blood-flow redistribution and neuroprotection after neonatal hypoxia-ischemia. Stroke 2014;45:850–6.
38. Fontaine RH, Olivier P, Massonneau V, et al. Vulnerability of white matter towards antenatal hypoxia is linked to a species-dependent regulation of glutamate receptor subunits. Proc Natl Acad Sci USA 2008;105:16779–84.
39. Bouslama M, Durand E, Chauvière L, Van den Bergh O, Gallego J. Olfactory classical conditioning in newborn mice. Behav Brain Res 2005;161:102–6.